Hindawi Publishing Corporation
Mathematical Problems in Engineering
Volume 2012, Article ID 568345, 14 pages
doi:10.1155/2012/568345

Research Article

Analytic Approximations for the Flows and Heat Transfer in Microchannels between Two Parallel Plates

A. El-Nahhas

Mathematics Department, Faculty of Science, Helwan University, Cairo 11795, Egypt

Correspondence should be addressed to A. El-Nahhas, aasayed35@yahoo.com

Received 19 October 2011; Revised 15 December 2011; Accepted 15 December 2011

Academic Editor: Anuar Ishak

We consider the nonlinear problem for the flow of Newtonian fluid in a microchannel between two parallel plates with the effects of velocity slip, viscous dissipation, and temperature jump at the wall. This problem is modelled by both the Navier-Stokes equation and energy equation with two thermal boundary conditions related to the two cases: the constant wall temperature (CWT) and the constant heat flux (CHF). The homotopy analysis method is applied via a polynomial exponential basis to obtain analytic approximations for this problem. A rarefaction effects on the velocity profile and the flow friction are investigated. Also, as a result of the application, the effects, on the Nusselt number Nu, with variation in Brinkman number Br and Knudsen number Kn for both (CWT) case and (CHF) case are discussed.

1. Introduction

Research on flow and heat transfer in microchannels has increased, recently, due to the developments in specific areas such as microfabrication technology, microdevices, Microelectromechanical Systems (MEMSs), the electronic industry, and the biomedical engineering. Microscale fluid flow and heat transfer has a different behaviour from that of macroscale case. At macroscale case, classical conservation equations are successfully coupled with the corresponding wall boundary conditions, usual no-slip for hydrodynamic boundary condition and no-temperature jump for thermal boundary condition. For a rarefied fluid flow at microscale a slip condition for the velocity and a jump condition for the temperature should be adopted. Viscous dissipation is another parameter that should be taking into account at microscale. Viscous dissipation changes the temperature by behaving like an energy source due to a power generation induced by the shear stress.

The Knudsen number Kn is the ratio of the fluid mean free path to the characteristic dimension in the flow field, and it determines the degree of rarefaction and the degree of the validity of continuum approach. For flows in continuum and slip regions, Eckert and Drake [1] indicated that there is a strong evidence to use the Navier-Stokes equations modified by boundary conditions. Beskok and Karniadakis [2] defined four different flow regimes based on the value of the Knudsen number: continuum flow (Kn < 0.001), slip flow (0.001 < Kn < 0.1), transition flow (0.1 < Kn < 10), and free molecular flow (Kn > 10). Liu et al. [3] and Arkilic et al. [4] pointed that the Navier-Stokes equations, when they are combined with slip-flow boundary conditions, give results for pressure drop and friction factor which are in agreement with the experimental data for some microchannel flows.

Gad-el-Hak [5] treated analysis for microchannel flows through study of microdevices fluid mechanics. Guo and Li [6] studied the size effects on microscale single-phase fluid flow and heat transfer. Wu and Cheng [7] studied the friction factor and convective heat transfer in smooth silicon microchannels of trapezoidal cross-section. Zhang et al. [8] validated the Navier-Stokes equations for slip flow with transition region. For recent studies in microchannel flows and heat transfer, see, for example, [9–15]. The homotopy analysis method presented by Liao [16–19] is a powerful tool for such kind of problems which have complicated and strong nonlinearity. This method does not depend on existence of small or large parameters in studied problems such as the perturbation methods [20–22], it does not use discretization of numerical methods, which have difficulties in case of the existence of singularities, and unlike other methods, such as Lyapunov's small parameter method [23] and the Adomian decomposition method [24–27], it has the ability to control the convergence for obtained approximations. Liao and other authors applied this method in a successful manner to various nonlinear applications in science and engineering. See, for example, [28–34]. To show the basic ideas and aspects of this method, let us consider the following:

$$N\left[g(r,t)\right] = 0, \tag{1.1}$$

where N is a nonlinear operator, g is unknown function, r is a vector of spatial variables, and t is the time. By means of the traditional concept of homotopy, Liao constructs the so-called zero-order deformation equation:

$$(1-q)L\left[\phi(r,t,q) - g_0(r,t)\right] = qhN\left[\phi(r,t,q)\right], \tag{1.2}$$

where $q\ \varepsilon\ [0,1]$ is an embedding parameter, L is an auxiliary linear operator, g_0 is an initial approximation for the unknown function g, and h is an auxiliary parameter. As q varies from 0 to 1, the solution of (1.2) varies from the initial approximation g_0 to the exact solution g of the nonlinear equation (1.1):

$$\phi(r,t,0) = g_0(r,t), \qquad \phi(r,t,1) = g(r,t). \tag{1.3}$$

Expanding $\phi(r,t,q)$ in Taylor series, with respect to q, one has

$$\phi(r,t,q) = g_0(r,t) + \sum_{m=1}^{\infty} g_m(r,t)q^m, \tag{1.4}$$

$$g_m(r,t) = \frac{1}{m!}\frac{\partial^m \phi(r,t,q)}{\partial q^m}\Big|_{q=0}. \tag{1.5}$$

If the parameter h is properly chosen such that the series (1.4) is convergent at $q = 1$, then from (1.3)

$$g(r,t) = g_0(r,t) + \sum_{m=1}^{\infty} g_m(r,t). \tag{1.6}$$

Differentiating the zero-order deformation equation (1.2) m times with respect to q, setting $q = 0$, and finally dividing by $m!$, we obtain the mth order deformation equation:

$$L\left[g_m(r,t) - \chi_m g_{m-1}(r,t)\right] = hP_m(r,t), \quad m \geq 1, \tag{1.7}$$

$$P_m(r,t) = \frac{1}{(m-1)!}\frac{\partial^{m-1} N\left[\phi(r,t,q)\right]}{\partial q^{m-1}}\Big|_{q=0}, \tag{1.8}$$

$$\chi_m = \begin{cases} 0, & m = 1, \\ 1, & m > 1. \end{cases} \tag{1.9}$$

The solutions $g_m(r,t), m \geq 1$, of (1.7) are called the mth deformations and can be computed by any symbolic software. The homotopy analysis method provides a freedom to choose L, g_0 and control the convergence, by the aid of the parameter h, to obtain analytic approximations in terms of suitable basis of functions.

2. Mathematical Formulation

The mathematical modelling for two-dimensional steady laminar slip flow in a microchannel between two parallel plates, with the consideration of Viscous dissipation, has the following form.

The continuity equation:

$$\frac{\partial u}{\partial x} + \frac{\partial v}{\partial y} = 0. \tag{2.1}$$

The Navier-Stokes equations:

$$u\frac{\partial u}{\partial x} + v\frac{\partial u}{\partial y} = -\frac{1}{\rho}\frac{\partial p}{\partial x} + \upsilon\left(\frac{\partial^2 u}{\partial x^2} + \frac{\partial^2 u}{\partial y^2}\right), \tag{2.2}$$

$$u\frac{\partial v}{\partial x} + v\frac{\partial v}{\partial y} = -\frac{1}{\rho}\frac{\partial p}{\partial y} + \upsilon\left(\frac{\partial^2 v}{\partial x^2} + \frac{\partial^2 v}{\partial y^2}\right). \tag{2.3}$$

The energy equation

$$u\frac{\partial T}{\partial x} + v\frac{\partial T}{\partial y} = \alpha\frac{\partial^2 T}{\partial y^2} + \frac{\upsilon}{Cp}\left(\frac{\partial u}{\partial y}\right)^2, \tag{2.4}$$

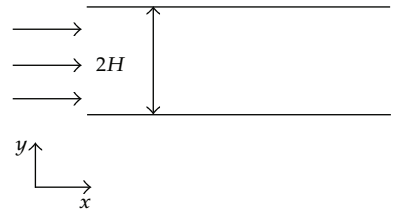

Figure 1: Microchannel between two parallel plates.

where in the previous equations, it is assumed that the inlet velocity and the inlet temperature are uniform, the distance between the two parallel plates is 2H (see Figure 1), and the tangential and thermal accommodation coefficients are taken to be unity. Also, u and v are velocity components, ρ is the density, p is the pressure, υ is the kinematic viscosity, T is the temperature, α is the thermal diffusivity, and C_p is the specific heat.

Equations (2.1)–(2.4) are subject to the following boundary conditions:

$$u = \ell \frac{\partial u}{\partial y}, \quad v = 0 \text{ at } y = 0, \qquad \frac{\partial u}{\partial y} = 0 \quad \text{at } y = H,$$

$$T - T_w = \ell \frac{\partial T}{\partial y} \quad \text{(for CWT)}, \qquad T - T_w = -\ell \frac{q_w}{\lambda} \quad \text{(for CHF) at } y = 0, \tag{2.5}$$

$$\frac{\partial T}{\partial y} = 0 \quad \text{at } y = H,$$

where ℓ is the molecular free path, T_w is the temperature at the wall, q_w is the heat flux at the wall, and λ is the thermal conductivity.

Using transformations of the form

$$\eta = \frac{1}{H} y, \qquad \psi = f(\eta) U x, \tag{2.6}$$

where ψ is a stream function and U is the inlet velocity, (2.3) can be reduced to

$$\frac{\partial}{\partial y}\left[\frac{\partial p}{\partial x}\right] = 0, \tag{2.7}$$

and hence from (2.7) we can write

$$-\frac{1}{\rho}\frac{\partial p}{\partial x} = Cx, \tag{2.8}$$

where C is a constant.

The mean velocity u_m has the following form:

$$u_m = \frac{1}{H}\int_0^H u\, dy = \frac{1}{H} f(1) U x. \tag{2.9}$$

Also, the mean temperature T_m has following the form:

$$T_m = \frac{1}{H}\int_0^H \left(\frac{u}{u_m}\right) T\,dy = \frac{1}{f(1)}\int_0^1 f'(\eta)T\,d\eta. \tag{2.10}$$

By the aid of (2.6), (2.8), and the following transformations:

$$\begin{aligned} \theta &= \left[\frac{H^2}{x^2}\right]\left[\frac{T-T_w}{T_m-T_w}\right] \quad \text{(for CWT)},\\ \theta &= \left[\frac{H^2}{x^2}\right]\left[\frac{T-T_w+\ell q_w/\lambda}{T_m-T_w+\ell q_w/\lambda}\right] \quad \text{(for CHF)}, \end{aligned} \tag{2.11}$$

equations (2.1)–(2.4) are transformed to the system of two equations:

$$\begin{aligned} f'''(\eta) - (\mathrm{Re})f'^2(\eta) + (\mathrm{Re})f(\eta)f''(\eta) + \varepsilon = 0,\\ \theta''(\eta) - (\mathrm{Br})f''^2(\eta) + (\mathrm{Pe})f(\eta)\theta'(\eta) - 2(\mathrm{Pe})f'(\eta)\theta(\eta) = 0, \end{aligned} \tag{2.12}$$

with the following boundary conditions:

$$\begin{aligned} &f'(0) - (\mathrm{Kn})f''(0) = 0, \qquad f(0) = 0, \qquad f''(1) = 0,\\ &\theta(0) - (\mathrm{Kn})\theta'(0) = 0 \quad \text{(for CWT)}, \qquad \theta(0) = 0 \quad \text{(for CHF)}, \qquad \theta'(1) = 0, \end{aligned} \tag{2.13}$$

where $\mathrm{Kn} = \ell/[2H]$ is the Knudsen number, $\mathrm{Br} = \mu\, U^2/[\lambda(T_w - T_m)]$ is the Brinkman number, μ is the dynamic viscosity, $\mathrm{Re} = UH/\upsilon$ is the Reynolds number, $\varepsilon = CH^3/[U\upsilon]$ and $\mathrm{Pe} = UH/\alpha$ is the Peclet number.

Not only (2.12) are strongly nonlinear but also they have linear boundary conditions. Poiseuille number is one of the most important parameters in fluid flow which is the product of friction factor and local Reynolds number. This number is denoted by Po and, based on the mean velocity [15], it can be given by

$$\mathrm{Po} = \frac{4f''(0)}{f(1)}. \tag{2.14}$$

The most important parameter in heat transfer is the ratio of convective to conductive heat transfer across the boundary which is called the Nusselt number. This number is denoted by Nu and, as in [15], analytic expressions for Nu can be drived for for both the (CWT) and (CHF) cases as follows:

$$\begin{aligned} \mathrm{Nu} &= \frac{2f(1)\theta'(0)}{\int_0^1 f'(\eta)\theta(\eta)\,d\eta} \quad \text{for (CWT) case},\\ \mathrm{Nu} &= \frac{2f(1)\theta'(0)}{\int_0^1 f'(\eta)\theta(\eta)\,d\eta - 2(\mathrm{Kn})f(1)\theta'(0)} \quad \text{for (CHF) case}. \end{aligned} \tag{2.15}$$

Here, we apply the homotopy analysis method via a polynomial exponential basis to get analytic approximations for solutions of (2.12)–(2.13), and then we use these approximations to discuss the rarefaction effects on velocity profile and flow friction (effects on Poiseuille number). Also, we use the expressions (2.15) to study the effects on the Nusselt number with the variations in Brinkman and Knudsen numbers.

3. Application of the Homotopy Analysis Method

Applying the homotopy analysis method on (2.12)–(2.13), we use the basis

$$\eta^m e^{n\eta}, \quad m, n \geq 0. \tag{3.1}$$

Also, we express the solutions by the rule of the following expressions:

$$f(\eta) = \sum_{n=1}^{\infty} \sum_{m=1}^{\infty} A_{n,m} \eta^m e^{n\eta}, \tag{3.2}$$

$$\theta(\eta) = \sum_{n=0}^{\infty} \sum_{m=0}^{\infty} B_{n,m} \eta^m e^{n\eta} \quad \text{for (CWT) case}, \tag{3.3}$$

$$\theta(\eta) = \sum_{n=1}^{\infty} \sum_{m=1}^{\infty} C_{n,m}\ \eta^m e^{n\eta} \quad \text{for (CHF) case}. \tag{3.4}$$

Viewing (2.12)–(2.13) and (3.1)–(3.4), we choose the initial approximations and the auxiliary linear operators as follows:

$$f_0(\eta) = 2(\mathrm{Kn})\eta e^{\eta} + (1 - 2\mathrm{Kn})\eta^2 e^{\eta} + \frac{1}{13}(8\mathrm{Kn} - 7)\eta^3 e^{\eta}, \tag{3.5}$$

$$\theta_0(\eta) = \mathrm{Kn} + \eta e^{\eta} - \frac{2}{3}\eta^2 e^{\eta} \quad \text{for (CWT) case}, \tag{3.6}$$

$$\theta_0(\eta) = \eta e^{\eta} - \frac{2}{3}\eta^2 e^{\eta} \quad \text{for (CHF) case}, \tag{3.7}$$

$$L_f = \frac{1}{3} e^{-\eta} \frac{\partial^3}{\partial \eta^3}, \tag{3.8}$$

$$L_\theta = \frac{1}{2} e^{-\eta} \frac{\partial^2}{\partial \eta^2}. \tag{3.9}$$

We construct the so-called zero-order deformation equations:

$$(1 - q) L_f \left[\phi(\eta, q) - f_0(\eta)\right] = h_f q N_f \left[\phi, \psi, q\right], \tag{3.10}$$

$$(1 - q) L_\theta \left[\psi(\eta, q) - \theta_0(\eta)\right] = h_\theta q N_\theta \left[\phi, \psi, q\right], \tag{3.11}$$

with the following conditions:

$$\frac{\partial\phi(\eta,q)}{\partial\eta}\Big|_{\eta=0} - (\mathrm{Kn})\frac{\partial^2\phi(\eta,q)}{\partial\eta^2}\Big|_{\eta=0} = 0, \quad \phi(0,q) = 0, \ \frac{\partial^2\phi(\eta,q)}{\partial\eta^2}\Big|_{\eta=1} = 0,$$
$$\psi(0,q) - (\mathrm{Kn})\frac{\partial\psi(\eta,q)}{\partial\eta}\Big|_{\eta=0} = 0 \quad (\text{for CWT}), \ \psi(0,q) = 0 \ (\text{for CHF}), \tag{3.12}$$
$$\frac{\partial\psi(\eta,q)}{\partial\eta}\Big|_{\eta=1} = 0,$$

where h_f and h_θ are auxiliary parameters and q is an embedding parameter that varies from 0 to 1. As q varies from 0 to, 1 the solution of (3.10)–(3.12) varies from the initial approximations to the exact solutions of (2.12)–(2.13). Thus we have

$$\phi(\eta,0) = f_0(\eta), \qquad \phi(\eta,1) = f(\eta), \qquad \psi(\eta,0) = \theta_0(\eta), \qquad \psi(\eta,1) = \theta(\eta). \tag{3.13}$$

The nonlinear operators N_f and N_θ in (3.10) and (3.11) are defined as

$$N_f[\phi,\psi,q] = \frac{\partial^3\phi}{\partial\eta^3} - (\mathrm{Re})\left(\frac{\partial\phi}{\partial\eta}\right)^2 + (\mathrm{Re})\phi\frac{\partial^2\phi}{\partial\eta^2} + \varepsilon,$$
$$N_\theta[\phi,\psi,q] = \frac{\partial^2\psi}{\partial\eta^2} - (\mathrm{Br})\left(\frac{\partial^2\phi}{\partial\eta^2}\right)^2 + (\mathrm{Pe})\phi\frac{\partial\psi}{\partial\eta} - 2(\mathrm{Pe})\frac{\partial\phi}{\partial\eta}\ \psi. \tag{3.14}$$

By Taylor's series, at $q = 0$, we have

$$\phi(\eta,q) = \phi(\eta,0) + \sum_{m=1}^{\infty} f_m(\eta)\ q^m,$$
$$\psi(\eta,q) = \psi(\eta,0) + \sum_{m=1}^{\infty} \theta_m(\eta)\ q^m, \tag{3.15}$$

where

$$f_m(\eta) = \frac{1}{m!}\frac{\partial^m\phi(\eta,q)}{\partial q^m}\Big|_{q=0}, \qquad \theta_m(\eta) = \frac{1}{m!}\frac{\partial^m\psi(\eta,q)}{\partial q^m}\Big|_{q=0}. \tag{3.16}$$

If the parameters h_f and h_θ are properly chosen such that the series (3.15) converge at $q = 1$, then from (3.13)

$$f(\eta) = f_0(\eta) + \sum_{m=1}^{\infty} f_m(\eta),$$
$$\theta(\eta) = \theta_0(\eta) + \sum_{m=1}^{\infty} \theta_m(\eta). \tag{3.17}$$

Differentiating the zero-order deformation equations (3.10) and (3.11) m times with respect to q, setting $q = 0$, and then dividing by $m!$, we obtain the mth order deformation equations:

$$\begin{aligned} L_f\left[f_m(\eta) - \chi_m f_{m-1}(\eta)\right] &= h_f P_m(\eta), \quad m \geq 1, \\ L_\theta\left[\theta_m(\eta) - \chi_m \theta_{m-1}(\eta)\right] &= h_\theta Q_m(\eta), \quad m \geq 1, \end{aligned} \tag{3.18}$$

where

$$\begin{aligned} P_m(\eta) &= f'''_{m-1}(\eta) - [\mathrm{Re}]\sum_{n=0}^{m-1} f'_n(\eta) f'_{m-1-n}(\eta) + [\mathrm{Re}]\sum_{n=0}^{m-1} f_n(\eta) f''_{m-1-n}(\eta) + \varepsilon(1-\chi_m), \\ Q_m(\eta) &= \theta''_{m-1}(\eta) - [\mathrm{Br}]\sum_{n=0}^{m-1} f''_n(\eta) f''_{m-1-n}(\eta) \\ &\quad + [\mathrm{Pe}]\sum_{n=0}^{m-1} f_n(\eta)\theta'_{m-1-n}(\eta) - 2[\mathrm{Pe}]\sum_{n=0}^{m-1} f'_n(\eta)\theta_{m-1-n}(\eta), \\ \chi_m &= \begin{cases} 0, & m = 1, \\ 1, & m > 1. \end{cases} \end{aligned} \tag{3.19}$$

The solutions of (3.18) are referred as the mth deformations, $m \geq 1$, and these deformations may satisfy the following conditions:

$$\begin{aligned} &\frac{\partial f_m(\eta)}{\partial \eta}\Big|_{\eta=0} - (\mathrm{Kn})\frac{\partial^2 f_m(\eta)}{\partial \eta^2}\Big|_{\eta=0} = 0, \quad f_m(0) = 0, \ \frac{\partial^2 f_m(\eta)}{\partial \eta^2}\Big|_{\eta=1} = 0, \\ &\theta_m(0) - (\mathrm{Kn})\frac{\partial \theta_m(\eta)}{\partial \eta}\Big|_{\eta=0} = 0 \quad (\text{for CWT}), \ \theta_m(0) = 0 \ (\text{for CHF}), \\ &\frac{\partial \theta_m(\eta)}{\partial \eta}\Big|_{\eta=1} = 0. \end{aligned} \tag{3.20}$$

The solutions of (3.18) can be obtained by a symbolic software such as Mathematica, and these solutions can be taken as

$$\begin{aligned} f_m(\eta) &= \sum_{n=1}^{2m+1}\sum_{k=1}^{2m+1} a_{m,n}^k \eta^k e^{n\eta}, \\ \theta_m(\eta) &= \sum_{n=0}^{2m+1}\sum_{k=0}^{2m+1} b_{m,n}^k \eta^k e^{n\eta} \quad \text{for (CWT) case}, \\ \theta_m(\eta) &= \sum_{n=1}^{2m+1}\sum_{k=1}^{2m+1} c_{m,n}^k \eta^k e^{n\eta} \quad \text{for (CHF) case}. \end{aligned} \tag{3.21}$$

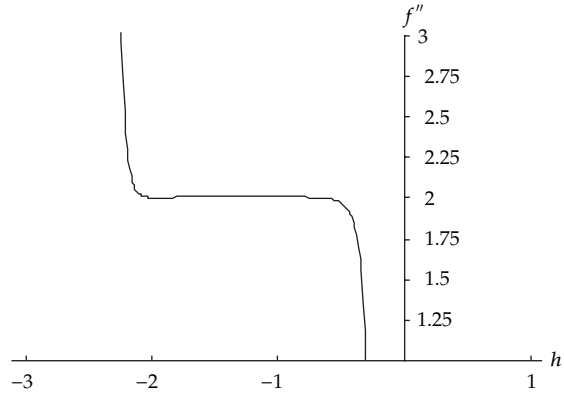

Figure 2: The h-curve for $f''(0)$ at Kn = 0.05, Br = 5, Pe = 0.5, and Re = 10.

For a best choice of h_f and h_θ, the Mth order approximations for the solutions of (2.12)–(2.13) are then

$$\begin{aligned} f(\eta) &= f_0(\eta) + \sum_{m=1}^{M} \sum_{n=1}^{2m+1} \sum_{k=1}^{2m+1} a_{m,n}^{k} \eta^k e^{n\eta}, \\ \theta(\eta) &= \theta_0(\eta) + \sum_{m=1}^{M} \sum_{n=0}^{2m+1} \sum_{k=0}^{2m+1} b_{m,n}^{k} \eta^k e^{n\eta} \quad \text{for (CWT) case,} \\ \theta(\eta) &= \theta_0(\eta) + \sum_{m=1}^{M} \sum_{n=1}^{2m+1} \sum_{k=1}^{2m+1} c_{m,n}^{k} \eta^k e^{n\eta} \quad \text{for (CHF) case.} \end{aligned} \tag{3.22}$$

The best values of parameters h_f and h_θ which control the convergence of the approximations (3.22) can be deduced by plotting the h-curve of $f''(0)$ and $\theta''(0)$ which takes a horizontal line through the position of convergence.

4. Results of the Application

Applying the homotopy analysis method for (2.12)–(2.13) up to the 10th order approximation it is found that it is best to take the control parameters h_f and h_θ such that $h_f = h_\theta = h = -1.2$ to get the best approximations for the solutions, as indicated in Figures 2, 3, and 4. In our study, Brinkman number Br and the Knudsen number Kn are the main parameters for heat and fluid flow in a microchannel. We study the interactive effects of these parameters for both the hydrodynamic and the thermal transport in the microchannel. We examine two different thermal boundary conditions at the wall of the microchannel: the constant wall temperature (CWT) and the constant heat flux (CHF).

Also, it is noted that Kn = 0 represents the macroscale case, while Kn > 0 holds for the microscale case and Br = 0 represents the case without effect of the viscous dissipation.

Figure 5 investigates the dimensionless velocity profile for no-slip and slip microchannel flow. When Kn = 0, the velocity increases from zero at wall to a maximum value (1.5) at plate centerline. The dimensionless velocity profile seems near parabolic. The velocity profile

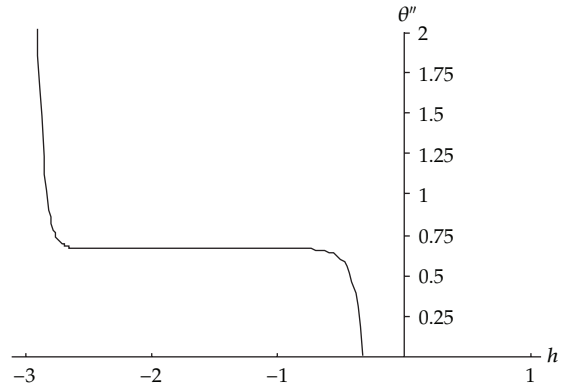

Figure 3: The h-curve for $\theta''(0)$ for CHF case at Kn = 0.05, Br = 5, Pe = 0.5, and Re = 10.

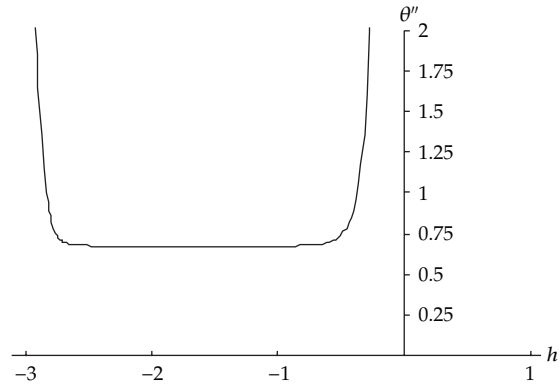

Figure 4: The h-curve for $\theta''(0)$ for CWT case at Kn = 0.05, Br = 5, Pe = 0.5, and Re = 10.

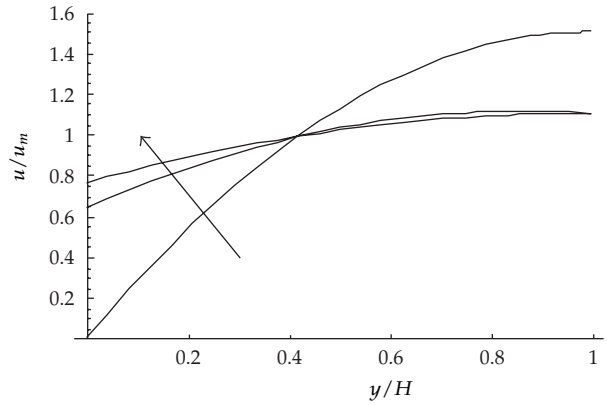

Figure 5: The dimensionless velocity profile for different values of Kn = 0, 0.05, 0.1.

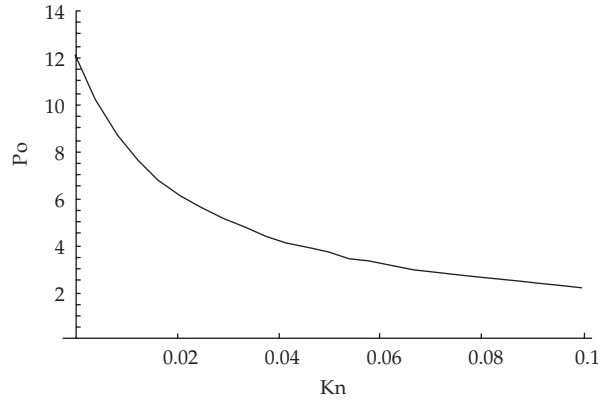

Figure 6: The Poiseuille number Po with continuous variation of Kn.

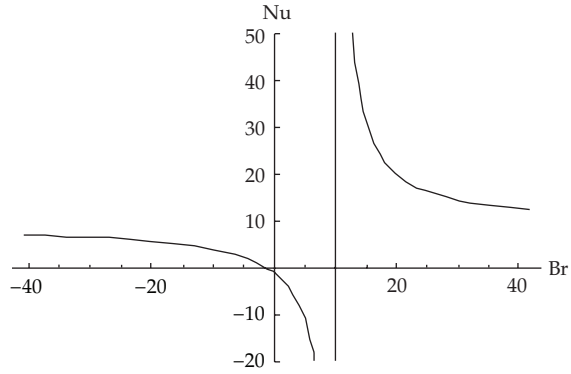

Figure 7: Effects on Nu with Br at Kn = 0 for CWT case.

for Kn = 0.05 and Kn = 0.1 are traced in this figure and it is remarked that all velocity profiles for the three cases of Kn intersect at one point. Figure 6 indicates the Poiseuille number Po with the continuous variation of the Knudsen number Kn. In this figure, the values of the Poiseuille number decrease gradually with the increase of Kn.

This is expected because the higher value of Kn implies larger slip and the higher velocity near the wall decreases the shear stress which causes the Po to drop further. This figure shows, also, that Po = 12 when Kn = 0 which agrees with the macroscale case and goes to an asymptotic value with the increasing of Kn. Figures 7 and 8 illustrate the effects on Nusselt number Nu, with variation in the Brinkman number Br and different values of Knudsen number Kn for the constant wall temperature (CWT) case. These figures seem to be a hyperbola for each Kn. In general, these figures show that the increase of Knudsen number Kn decreases the Nusselt number Nu due to the temperature jump at the wall. If the Brinkman number Br takes positive values, then this corresponds to what is called wall heating case. For this case, the wall temperature is greater than that of the bulk fluid. For this case it is noticed that Nu decreases as Br increases. Also, the value of Br indicates the effects of the viscous dissipation. Viscous dissipation increases the temperature of the bulk fluid especially near the wall, because the highest shear rate occurs in this region. This effect causes

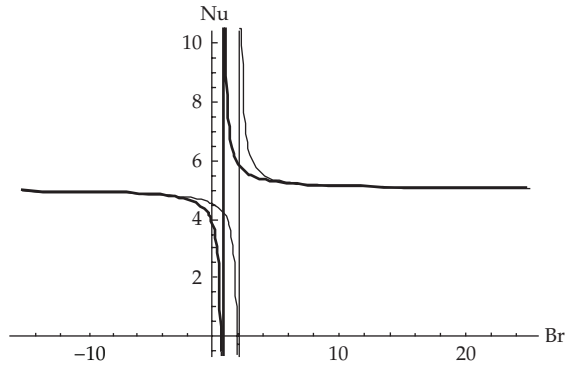

Figure 8: Effects on Nu with Br at Kn = 0.05 (thin line) and 0.1 (solid line) for CWT case.

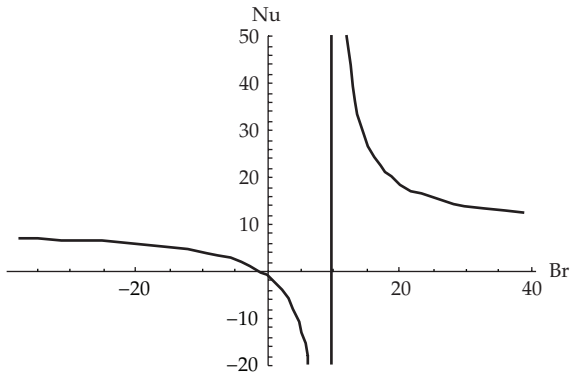

Figure 9: Effects on Nu with Br at Kn = 0 for CHF case.

the temperature difference between wall and the bulk fluid decrease. The extra increasing of Br yields that the heat supplied by the wall into the fluid is balanced with the internal heat due to the viscous heating and hence the Nu reaches an asymptotic value. Also, for wall cooling case when Br takes negative values, the Nu reaches an asymptotic value with the increasing of Br in the negative direction. Figures 9 and 10 depict the effects on the Nusselt number Nu, with the variation in Brinkman number Br and different values of Knudsen number Kn for the constant heat flux (CHF) case. The effects on Nu are very similar to the case of constant wall temperature (CWT). This similarity can be expected from the similarity of the formulae (2.15) of the Nusselt number Nu and also from the similarity of the initials of the temperature profile in (3.6) and (3.7).

5. Conclusion

In this paper the homotopy analysis method was applied via a polynomial exponential basis to obtain analytic approximations for the nonlinear problem of the flow fluid in a microchannel between two parallel plates taking into account the effects of velocity slip, viscous dissipation, and temperature jump at the wall. As a result of this application, the rarefied effects on the velocity profile and the flow friction are studied and also effects on the

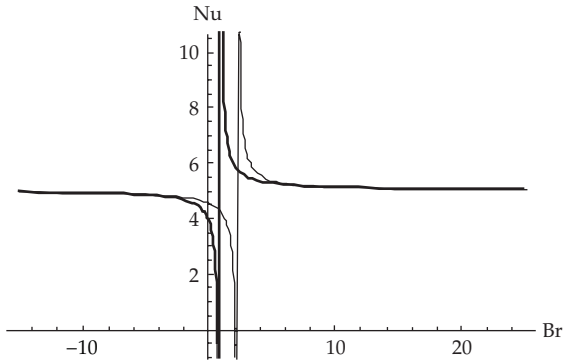

Figure 10: Effects on Nu with Br at Kn = 0.05 (thin line) and 0.1 (solid line) for CHF case.

Nusselt number with the variation in Brinkman and Knudsen numbers are discussed for both the constant wall temperature (CWT) and the constant heat flux (CHF). Also, the application proved the great ability and flexibility of this method to treat the strongly nonlinear problems which have linear boundary conditions via any suitable set of continuous functional basis.

Acknowledgment

The author thanks the anonymous reviewers for their comments and suggestions to enhance this work.

References

[1] E. G. R. Eckert and R. M. Drake Jr, *Analysis of Heat and Mass Transfer*, McGraw-Hill, New York, NY, USA, 1972.

[2] A. Beskok and G. E. Karniadakis, "Simulation of heat and momentum transfer in complex micro-geometries," *AIAA Journal of Thermophysics and Heat Transfer*, vol. 8, no. 4, pp. 355–370, 1994.

[3] J. Q. Liu, Y. C. Tai, and C. M. Ho, "MEMS for pressure distribution studies of gaseous flows in microchannels," in *Proceedings of the IEEE Micro Electro Mechanical Systems*, pp. 209–215, 1995.

[4] E. B. Arkilic, K. S. Breuer, and M. A. Schmidt, "Gaseous flow in microchannels," in *Proceedings of the 1st ASME Symposium on Application of Micro-Fabrication to Fluid Mechanics*, pp. 57–65, American Society of Mechanical Engineers, Chicago, Ill, USA, 1994.

[5] M. Gad-el-Hak, "Fluid mechanics of microdevices-the freeman scholar lecture," *Journal of Fluids Engineering*, vol. 121, no. 1, pp. 5–33, 1999.

[6] Z. Y. Guo and Z. X. Li, "Size effect on microscale single-phase flow and heat transfer," *International Journal of Heat and Mass Transfer*, vol. 46, no. 1, pp. 149–159, 2003.

[7] H. Y. Wu and P. Cheng, "An experimental study of convective heat transfer in silicon microchannels with different surface conditions," *International Journal of Heat and Mass Transfer*, vol. 46, no. 14, pp. 2547–2556, 2003.

[8] T. T. Zhang, L. Jia, and Z. C. Wang, "Validation of Navier-Stokes equations for slip flow analysis within transition region," *International Journal of Heat and Mass Transfer*, vol. 51, no. 25-26, pp. 6323–6327, 2008.

[9] Y. Zhang, R. Qin, and D. R. Emerson, "Lattice Boltzmann simulation of rarefied gas flows in microchannels," *Physical Review E*, vol. 71, no. 4, pp. 047702/1–047702/4, 2005.

[10] G. H. Tang, W. Q. Tao, and Y. L. He, "Lattice Boltzmann method for gaseous microflows using kinetic theory boundary conditions," *Physics of Fluids*, vol. 17, no. 5, Article ID 058101, pp. 1–4, 2005.

[11] G. Hetsroni, A. Mosyak, E. Pogrebnyak, and L. P. Yarin, "Fluid flow in micro-channels," *International Journal of Heat and Mass Transfer*, vol. 48, no. 10, pp. 1982–1998, 2005.

[12] O. Aydin and M. Avcı, "Heat and fluid flow characteristics of gases in micropipes," *International Journal of Heat and Mass Transfer*, vol. 49, no. 9-10, pp. 1723–1730, 2006.

[13] O. Aydın and M. Avcı, "Analysis of laminar heat transfer in micro-Poiseuille flow," *International Journal of Thermal Sciences*, vol. 46, no. 1, pp. 30–37, 2007.

[14] J. van Rij, T. Harman, and T. Ameel, "The effect of creep flow on two-dimensional isoflux microchannels," *International Journal of Thermal Sciences*, vol. 46, no. 11, pp. 1095–1103, 2007.

[15] Z. C. Wang, D. W. Tang, and X. G. Hu, "Similarity solutions for flows and heat transfer in microchannels between two parallel plates," *International Journal of Heat and Mass Transfer*, vol. 54, no. 11-12, pp. 2349–2354, 2011.

[16] S. J. Liao, *The proposed homotopy analysis technique for the solutions of nonlinear problems*, Ph.D. thesis, Jiao Tong University, Shanghai, China, 1992.

[17] S. J. Liao, "An explicit, totally analytic approximate solution for Blasius viscous flow problems," *International Journal of Non-Linear Mechanics*, vol. 34, no. 4, pp. 759–778, 1999.

[18] S. J. Liao, "An analytic approximation of the drag coefficient for the viscous flow past a sphere," *International Journal of Non-Linear Mechanics*, vol. 37, no. 1, pp. 1–18, 2002.

[19] S. Liao, *Beyond Perturbation: Introduction to Homotopy Analysis Method*, Chapman & Hall/CRC Press, Boca Raton, Fla, USA, 2003.

[20] J. D. Cole, *Perturbation Methods in Applied Mathematics*, Blaisdell Publishing Company, Waltham, Mass, USA, 1968.

[21] A. W. Bush, *Perturbation Methods For Engineers and Scientists*, Library of Engineering Mathematics, CRC Press, Boca Raton, Fla, USA, 1992.

[22] A. H. Nayfeh, *Perturbation Methods*, John Wiley & Sons, New York, NY, USA, 2000.

[23] A. M. Lyapunov, *The General Problem of the Stability of Motion*, Taylor & Francis, London, UK, 1992.

[24] G. Adomian, "A review of the decomposition method in applied mathematics," *Journal of Mathematical Analysis and Applications*, vol. 135, no. 2, pp. 501–544, 1988.

[25] G. Adomian, "A review of the decomposition method and some recent results for nonlinear equations," *Computers & Mathematics with Applications*, vol. 21, no. 5, pp. 101–127, 1991.

[26] G. Adomian, "Solution of physical problems by decomposition," *Computers & Mathematics with Applications*, vol. 27, no. 9-10, pp. 145–154, 1994.

[27] G. Adomian, *Solving Frontier Problems of Physics: The Decomposition Method*, vol. 60, Kluwer Academic, Boston, Mass, USA, 1994.

[28] S. J. Liao, "An explicit analytic solution to the Thomas-Fermi equation," *Applied Mathematics and Computation*, vol. 144, no. 2-3, pp. 495–506, 2003.

[29] S. J. Liao, "Comparison between the homotopy analysis method and homotopy perturbation method," *Applied Mathematics and Computation*, vol. 169, no. 2, pp. 1186–1194, 2005.

[30] S. J. Liao, J. Su, and A. T. Chwang, "Series solutions for a nonlinear model of combined convective and radiative cooling of a spherical body," *International Journal of Heat and Mass Transfer*, vol. 49, no. 15-16, pp. 2437–2445, 2006.

[31] S. J. Liao and Y. Tan, "A general approach to obtain series solutions of nonlinear differential equations," *Studies in Applied Mathematics*, vol. 119, no. 4, pp. 297–354, 2007.

[32] J. Cheng, S. Liao, R. N. Mohapatra, and K. Vajravelu, "Series solutions of nano boundary layer flows by means of the homotopy analysis method," *Journal of Mathematical Analysis and Applications*, vol. 343, no. 1, pp. 233–245, 2008.

[33] S. J. Liao, "An optimal homotopy-analysis approach for strongly nonlinear differential equations," *Communications in Nonlinear Science and Numerical Simulation*, vol. 15, no. 8, pp. 2003–2016, 2010.

[34] N. Kousar and S. Liao, "Unsteady non-similarity boundary-layer flows caused by an impulsively stretching flat sheet," *Nonlinear Analysis. Real World Applications*, vol. 12, no. 1, pp. 333–342, 2011.